Research Article

Li-Fang Zhao and Wei Zhang*

Fourier spectral method for the fractional-in-space coupled Whitham–Broer–Kaup equations on unbounded domain

https://doi.org/10.1515/phys-2024-0071
received February 28, 2024; accepted July 19, 2024

Abstract: Due to the nonlocality of fractional derivatives, the numerical methods for solving nonlinear fractional Whitham–Broer–Kaup (WBK) equations are time-consuming and tedious. Therefore, it is a research hotspot to explore the numerical solution of fractional-order WBK equation. The main goal of this study is to provide an efficient method for the fractional-in-space coupled WBK equations on unbounded domain and discover some novel anomalous transmission behaviors. First, the numerical solution is compared with the exact solution to determine the validity of the proposed method on large time-spatial domain. Then, anomalous transmission of waves propagation of the fractional WBK equation is numerically simulated, and the influence of different fractional-order derivatives on wave propagation of the WBK equation is researched. Some novel anomalous transmission behaviors of wave propagation of the fractional WBK equation on unbounded domain are shown.

Keywords: space fractional coupled Whitham–Broer–Kaup equation, fractal anomalous transmission, waves propagation, numerical simulation

1 Introduction

We consider the following fractional-in-space Whitham–Broer–Kaup (WBK) equation [1–3]:

$$\begin{cases} \mathbf{u}_t + \mathbf{u}D_x^{\alpha_1}\mathbf{u} + D_x^{\alpha_2}\mathbf{v} + \beta D_x^{2\alpha_3}\mathbf{u} = 0, \\ \mathbf{v}_t + D_x^{\alpha_1}(\mathbf{vu}) + \gamma D_x^{3\alpha_4}\mathbf{u} - \beta D_x^{2\alpha_3}\mathbf{v} = 0, \\ \mathbf{u}(x,0) = \mathbf{u}_0(x), \mathbf{v}(x,0) = \mathbf{v}_0(x), x \in R, \\ |\mathbf{u}(x,t)| \to 0, |\mathbf{v}(x,t)| \to 0, |x| \to \infty, 0 < t \le T. \end{cases} \tag{1}$$

The fractional WBK equation describes the dispersive long wave in shallow water. The field of horizontal velocity is represented by $\mathbf{u}(x,t)$, and $\mathbf{v}(x,t)$ is the height that deviates from the equilibrium position of the liquid. $D_x^{\alpha}\mathbf{u}$ denote Caputo fractional derivative operator. $0 < \alpha_i \le 1$ represents the order of the fractional derivative. β and γ are constants that represent different diffusion powers.

Definition 1.1. The Caputo fractional derivative of $\alpha > 0$ order is defined as

$$ {}_aD_x^{\alpha}\mathbf{u}(x) = \begin{cases} \dfrac{1}{\Gamma(m-\alpha)}\displaystyle\int_a^x (x-\tau)^{m-\alpha-1}\frac{\mathrm{d}^m\mathbf{u}(\tau)}{\mathrm{d}\tau^m}\mathrm{d}\tau, \\ m-1 < \alpha < m, \\ \dfrac{\mathrm{d}^m}{\mathrm{d}x^m}\mathbf{u}(x), \qquad\qquad \alpha = m. \end{cases} \tag{2}$$

If $\alpha_i = 1$, the fractional WBK Eq. (1) reduces to the following integer WBK equations:

$$\begin{cases} \mathbf{u}_t + \mathbf{u}\mathbf{u}_x + \mathbf{v}_x + \beta\mathbf{u}_{xx} = 0, \\ \mathbf{v}_t + (\mathbf{vu})_x + \gamma\mathbf{u}_{xxx} - \beta\mathbf{v}_{xx} = 0. \end{cases} \tag{3}$$

If $\beta = 0$ and $\gamma = 1$, the WBK Eq. (3) reduces to the variant Boussinesq equations [4,5]

$$\begin{cases} \mathbf{u}_t + \mathbf{u}\mathbf{u}_x + \mathbf{v}_x = 0, \\ \mathbf{v}_t + (\mathbf{vu})_x + \mathbf{u}_{xxx} = 0. \end{cases} \tag{4}$$

If $\beta \neq 0$ and $\gamma = 0$, the WBK Eq. (3) reduces to the approximate long water wave equations [4,5] in the form

$$\begin{cases} \mathbf{u}_t + \mathbf{u}\mathbf{u}_x + \mathbf{v}_x + \beta\mathbf{u}_{xx} = 0, \\ \mathbf{v}_t + (\mathbf{vu})_x - \beta\mathbf{v}_{xx} = 0. \end{cases} \tag{5}$$

For the fractional WBK Eq. (1), the expansion method is applied by Yaslan [1] to obtain some analytic solutions of

* **Corresponding author: Wei Zhang,** Institute of Economics and Management, Jining Normal University, 012000, Ulanqab, China, e-mail: jnsfxyzw@163.com
Li-Fang Zhao: College of Physics and Electronic Information Engineering, Jining Normal University, 012000, Ulanqab, China

the fractional-in-space–time WBK equations. A general ansätz and the improved fractional sub-equation method are applied by Guo *et al.* [2] to construct the analytical solutions of the space–time fractional WBK equations. The enhanced extended tanh-function technique was used by Zaman *et al.* [3] to obtain the analytical behavior of soliton solutions to the couple-type fractional-order WBK equations. Ghehsareh *et al.* [6] used Lie symmetry analysis and conservation laws for time fractional coupled WBK equation. Saha [7] used a novel method to obtain some travelling wave solutions [8] of fractional WBK equation. The Laplace transform combined with Adomian decomposition method was applied by Ali *et al.* [9] to obtain an analytic approximate solution of nonlinear fractional WBK equations.

For the integer WBK Eq. (3), some scholars applied various methods and obtained analytical solutions. For example, Chen *et al.* [10] applied the generalized method and obtained nine families of solutions. Abdou [11] applied the extended tanh method and obtained nine families of solutions of the WBK equation. Guo *et al.* [4] applied the G/G-function method and found four families of solutions of the WBK equation. Song *et al.* [12] applied the bifurcation method and found 13 families of solutions of the WBK equation. Xu and Li [13] used the improved auxiliary equation method and obtained four families of solutions of the WBK equation. Zheng *et al.* [5] applied the Exp-function method and obtained seven families of solutions of the WBK equation. Lin *et al.* [14] derived types of solutions of the WBK equation *via* the rational transformation. Lei *et al.* [15] and Xu [16] used the Gauge transformation and the Darboux transformation, respectively, and found multi-soliton solutions of the WBK equation. Fan and Zhang [17] applied the Backlund transformation to handle the WBK equations and found three families of solutions of the WBK equation. Yan and Zhang [18] used the Riccati transformation and found 12 families of solutions of the WBK equation. Xie *et al.* [19] used hyperbolic function method and obtained some solitary wave solutions of the WBK equation. Xu *et al.* [20] applied the extended tanh-function method and obtained nine families of solutions of the WBK equation. Several numerical methods have been applied for the solution of the integer WBK Eq. (3). The Exp-function method was used for the WBK equation and with the help of symbolic computation, several kinds of solitary wave solutions of the WBK equation were obtained by Zheng and Shan [21]. El-Sayed and Kaya [22] had presented explicit and numerical traveling wave solutions of the WBK equations in the form of an easily computable convergent power series. The Homotopy perturbation method was used for computing the coupled WBK shallow water by Ganji *et al.* [23].

Unlike integer WBK equations, fractional WBK equations have nonlocality and singularity, sometimes even involve space–time coupling which bring many difficulties and challenges in analysis, and numerical methods. Although there are some numerical methods for fractional differential equations, such as difference method [24–26], reproducing kernel method [27], barycentric interpolation collocation method [28], spectral method [29], and so on, Ning and Wang used the Fourier spectral method to investigate a class of fractional KdV-modified KdV equation [30], KdV–Burgers equation [31], FitzHugh–Nagumo model [32], pattern dynamics behavior of a fractional vegetation–water model [33], Gray–Scott model [34], and Ginzburg–Landau equation [35]. The numerical solutions of fractional WBK equations are rarely found.

In general, the Fourier spectral method is far more accurate than the finite difference method and the finite element method. Due to the continuous development of fast Fourier transform, the calculation amount of the Fourier spectral method is less and less. In general, when using the Fourier spectral method to solve partial differential equations (PDEs), it has the characteristics of small calculation amount, especially for more than two-dimensional problems. In order to improve the accuracy, the finite difference method must set enough grid nodes to solve the partial differential equation, so as to increase the calculation amount, while the Fourier spectral method generally does not need to take too many nodes to get a more high-precision solution. However, it is important to note that the Fourier spectral method solves PDEs with periodic boundary conditions. For some PDEs with aperiodic boundary conditions, how to ensure that the value at the boundary has little effect on the whole solution or that the value at the boundary is always a specific constant is a problem worth thinking about.

In this study, we present a numerical solution of nonlinear fractional-in-space WBK equations to study the propagation and interaction behavior of the fractional WBK equations on unbounded domain. Comparisons are made between the numerical and exact solutions, and it is found that the method is a satisfactory and efficient algorithm for capturing the propagation of the fractional-in-space WBK equations on unbounded domain. Experimental findings indicate that the proposed method is easy to implement, effective and convenient in the long-time simulation for solving the fractional-in-space WBK equations on unbounded domain. The influence of fractional derivative on fractional WBK equations and some of the anomalous bi-directional propagation behaviors of long waves over shallow water for fractional WBK equations is observed. In the experiment, we observe the propagation behaviors of fractional WBK equations which are unlike any that have been previously obtained in numerical studies.

2 Description of numerical method

The Fourier transform $\mathbb{F}_x(\mathbf{u}(x,t))$ of $\mathbf{u}(x,t)$ about spatial variable x is

$$\hat{\mathbf{u}}(\kappa,t)=\mathbb{F}_x(\mathbf{u}(x,t))=\int_{-\infty}^{\infty}\mathbf{u}(x,t)e^{-i\kappa x}\mathrm{d}x, \tag{6}$$

and the famous inverse Fourier transform $\mathbb{F}_\kappa^{-1}(\hat{\mathbf{u}}(\kappa,t))$ of $\hat{\mathbf{u}}(\kappa,t)$ about variable κ is

$$\mathbf{u}(x,t)=\mathbb{F}_\kappa^{-1}(\hat{\mathbf{u}}(\kappa,t))=\frac{1}{2\pi}\int_{-\infty}^{\infty}\hat{\mathbf{u}}(\kappa,t)e^{i\kappa x}\mathrm{d}\kappa. \tag{7}$$

Theorem 2.1. *When $a=-\infty$, Fourier transform of Caputo fractional derivative of α order is*

$$\begin{aligned}\mathbb{F}_x[{}_{-\infty}D_x^\alpha\mathbf{u}(x)]&=\mathbb{F}_x\left[\frac{1}{\Gamma(m-\alpha)}\int_{-\infty}^{x}(x-\tau)^{m-\alpha-1}\frac{\mathrm{d}^m\mathbf{u}(\tau)}{\mathrm{d}\tau^m}\mathrm{d}\tau\right]\\&=(i\kappa)^\alpha\hat{\mathbf{u}}(\kappa).\end{aligned} \tag{8}$$

Proof. Note

$$h_+(x)=\begin{cases}\dfrac{x^{m-\alpha-1}}{\Gamma(m-\alpha)}, & x>0,\\ 0, & x\le 0.\end{cases} \tag{9}$$

So,

$$\begin{aligned}&\mathbb{F}_x[{}_{-\infty}D_x^\alpha\mathbf{u}(x)]\\&=\mathbb{F}_x\left[\frac{1}{\Gamma(m-\alpha)}\int_{-\infty}^{x}(x-\tau)^{m-\alpha-1}\frac{\mathrm{d}^m\mathbf{u}(\tau)}{\mathrm{d}\tau^m}\mathrm{d}\tau\right]\\&=\mathbb{F}_x\left[h_+(x)*\frac{\mathrm{d}^m\mathbf{u}(\tau)}{\mathrm{d}\tau^m}\right]\\&=\mathbb{F}_x[h_+(x)]\mathbb{F}_x\left[\frac{\mathrm{d}^m\mathbf{u}(\tau)}{\mathrm{d}\tau^m}\right]\\&=(i\kappa)^{\alpha-m}(i\kappa)^m\hat{\mathbf{u}}(\kappa)\\&=(i\kappa)^\alpha\hat{\mathbf{u}}(\kappa).\square\end{aligned} \tag{10}$$

The famous Fourier transform $\mathbb{F}_x(\mathbf{u}(x,t))$ and the inverse Fourier transform $\mathbb{F}_\kappa^{-1}(\hat{\mathbf{u}}(\kappa,t))$ have the following conclusion:

$$\begin{aligned}&\mathbb{F}_x(D_x^\alpha\mathbf{u}(x,t))=(i\kappa)^\alpha\hat{\mathbf{u}}(\kappa,t),\\&D_x^\alpha\mathbf{u}(x,t)=\mathbb{F}_\kappa^{-1}((i\kappa)^\alpha\hat{\mathbf{u}}(\kappa,t)).\end{aligned} \tag{11}$$

Fourier spectral method is developed for the periodic initial value problem [29,31]. By using Fourier transform for Eq. (1) in space domain, Eq. (1) can be written as

$$\begin{cases}\dfrac{\mathrm{d}\hat{\mathbf{u}}}{\mathrm{d}t}=-\mathbb{F}_x[\mathbf{u}\mathbb{F}_k^{-1}((i\kappa)^{\alpha_1}\hat{\mathbf{u}})]+(i\kappa)^{\alpha_2}\hat{\mathbf{v}}+\beta(i\kappa)^{2\alpha_3}\hat{\mathbf{u}},\\ \dfrac{\mathrm{d}\hat{\mathbf{v}}}{\mathrm{d}t}=-\mathbb{F}_x[\mathbf{v}\mathbb{F}_k^{-1}((i\kappa)^{\alpha_1}\hat{\mathbf{u}})]+\mathbb{F}[\mathbf{u}F^{-1}((i\kappa)^{\alpha_1}\hat{\mathbf{v}})]\\ \qquad\qquad+\gamma(i\kappa)^{3\alpha_4}\hat{\mathbf{u}}-\beta(i\kappa)^{2\alpha_3}\hat{\mathbf{v}},\\ \hat{\mathbf{u}}(\kappa,0)=\hat{\mathbf{u}}_0(\kappa),\\ \hat{\mathbf{v}}(\kappa,0)=\hat{\mathbf{v}}_0(\kappa),\end{cases} \tag{12}$$

where $i^2=-1$, $\mathbb{F}_x$ represents the Fourier transform, and $\mathbb{F}_\kappa^{-1}$ denotes the inverse Fourier transform.

Note that for the above formula to hold, it is necessary to ensure that $|\mathbf{u}(x,t)|\to 0$, $|x|\to\infty$, $0<t\le T$, and the speed of approaching 0 must be greater than the exponential rate to ensure that the boundary term is 0. In the actual numerical calculation, we call the fftshift function in MATLAB to calculate, rather than directly using the definition of the Fourier transform to calculate. The spatial domain is $[-L/2,L/2]$ and the spatial step size $h=L/N$, and N is a natural number. The fast Fourier transform has been hailed as one of the greatest algorithms of the twentieth century. The arithmetic of the discrete Fourier transform algorithm is $O(N^2)$. The fast Fourier transform reduces the computation to $O(N\log N)$. However, in order to obtain a high speed of operation, the number of elements of the sequence to be transformed must be 2^N formal.

For convenience of expression, we denote

$$\begin{cases}\mathbf{U}=(\hat{\mathbf{u}}(\kappa,t),\hat{\mathbf{v}}(\kappa,t))^T,\\ H(t,\mathbf{U})=(h_1(\hat{\mathbf{u}}_0(t),\hat{\mathbf{v}}_0(t),t),h_2(\hat{\mathbf{u}}_0(t),\hat{\mathbf{v}}_0(t),t))^T,\\ \mathbf{U}_0=(\hat{\mathbf{u}}_0(\kappa),\hat{\mathbf{v}}_0(\kappa))^T,\end{cases} \tag{13}$$

where $h_1(\hat{\mathbf{u}},\hat{\mathbf{v}},t)=-\mathbb{F}_x[\mathbf{u}\mathbb{F}_k^{-1}((i\kappa)^{\alpha_1}\hat{\mathbf{u}})]+(i\kappa)^{\alpha_2}\hat{\mathbf{v}}+\beta(i\kappa)^{2\alpha_3}\hat{\mathbf{u}}$, $h_2(\hat{\mathbf{u}},\hat{\mathbf{v}},t)=-\mathbb{F}_x[\mathbf{v}\mathbb{F}_k^{-1}((i\kappa)^{\alpha_1}\hat{\mathbf{u}})]+\mathbb{F}[\mathbf{u}F^{-1}((i\kappa)^{\alpha_1}\hat{\mathbf{v}})]+\gamma(i\kappa)^{3\alpha_4}\hat{\mathbf{u}}-\beta(i\kappa)^{2\alpha_3}\hat{\mathbf{v}}$.

Eq. (12) is reduced to a system of ordinary differential equations with time differentiation

$$\begin{cases}\dfrac{\mathrm{d}\mathbf{U}}{\mathrm{d}t}=H(t,\mathbf{U}),\\ \mathbf{U}(\kappa,0)=\mathbf{U}_0.\end{cases} \tag{14}$$

Then, the Runge–Kutta method is used to solve Eq. (14), and the form is as follows:

$$\begin{cases}\mathbf{U}_{n+1}=\mathbf{U}_n+\dfrac{h}{6}(K_1+4K_2+K_3),\\ K_1=H(t_n,\mathbf{U}_n),\\ K_2=H\left(t_n+\dfrac{h}{2},\mathbf{U}_n+\dfrac{hK_1}{2}\right),\\ K_3=H(t_n+h,\mathbf{U}_n-hK_1+2hK_2),\end{cases} \tag{15}$$

where h is the step-size.

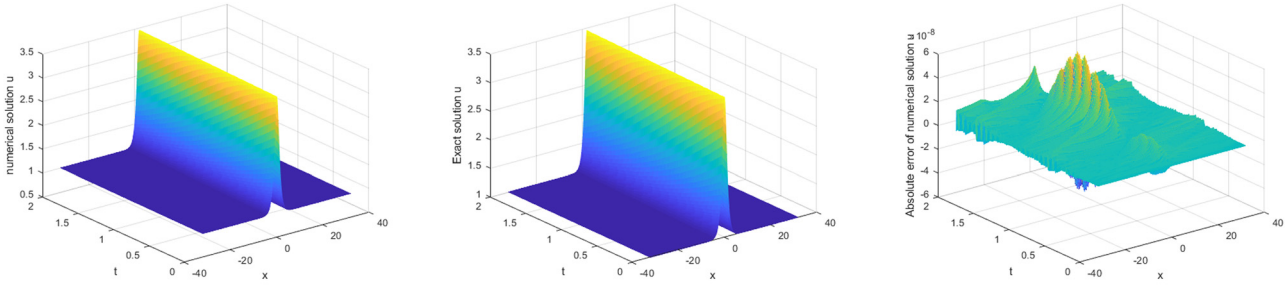

Figure 1: Comparison of numerical and exact solutions at $c = 1, a = 1, \gamma = 2, \beta = 0.9, L = 64, N = 512$. (a) Numerical solution $\mathbf{u}$, (b) exact solution $\mathbf{u}$, and (c) absolute error of $\mathbf{u}$.

Theorem 2.2. *If incremental function* $\Psi(\mathbf{U}, t, h) = \frac{1}{6}(H(t, \mathbf{U}) + 4H(t + \frac{h}{2}, \mathbf{U} + \frac{h}{2}H(t, \mathbf{U})) + H(t + h, \mathbf{U} - hH(t, \mathbf{U}) + 2H(t + \frac{h}{2}, \mathbf{U} + \frac{h}{2}hH(t, \mathbf{U}))))$ *is a continuous function on* $0 \le t \le T, -\infty \le \mathbf{U} \le \infty$ *satisfies the local Lipschitz condition about* $\mathbf{U}$,

$$|\Psi(t, U, h) - \Psi(t, \tilde{U}, h)| \le L_\Psi |U - \tilde{U}|, \tag{16}$$

then the solution of Eq. (14)*is well posed, the present method is stable and convergent, and the solution has the following error estimation form*:

$$|\mathbf{U}_n - \mathbf{U}(t_n)| \le \frac{Dh^3}{L_\Psi}(e^{L_\Psi T} - 1) + e^{L_\Psi T}|E_0|, \tag{17}$$

where L_Ψ *is the Lipschitz coefficient.*

Finally, we find the numerical solution using the fast inverse discrete Fourier Transform. In the actual numerical calculation, we call the ifftshift function in MATLAB to calculate, rather than directly using the definition of the fast inverse discrete Fourier Transform to calculate. In matlab, the functions that call the Fourier transform and inverse transformation are fft(u) and ifft(u).

The spectral method is essentially an extension of the method of separating variables. For periodic boundary conditions, it is convenient to use Fourier series and harmonic series. The accuracy of spectral methods generally depends on the number of terms of the series expansion. Spectral methods generally do not need to take more nodes.

3 Numerical simulation

Experiment: In Eq. (1), subject to the initial condition $\mathbf{u}_0(x) = c + \sqrt{6}\,\mathrm{sech}\frac{\sqrt{3}cx}{\sqrt{-2(\gamma+\beta^2)}}$, $\mathbf{v}_0(x) = cu - \frac{1}{2}u^2 - \beta u_x + c^2$. In this case, the corresponding exact solution is

$$\begin{cases} \mathbf{u}(\xi) = c + \sqrt{6}\,\mathrm{sech}\dfrac{\sqrt{3}c\xi}{\sqrt{-2(\gamma+\beta^2)}}, \\ \mathbf{v}(\xi) = cu(\xi) - \dfrac{1}{2}u^2(\xi) - \beta u_\xi(\xi) + c^2, \end{cases} \tag{18}$$

where $\gamma + \beta^2 < 0, \xi = x - ct$.

In order to confirm the validity of Fourier spectral method for the fractional-in-space coupled WBK equation, we

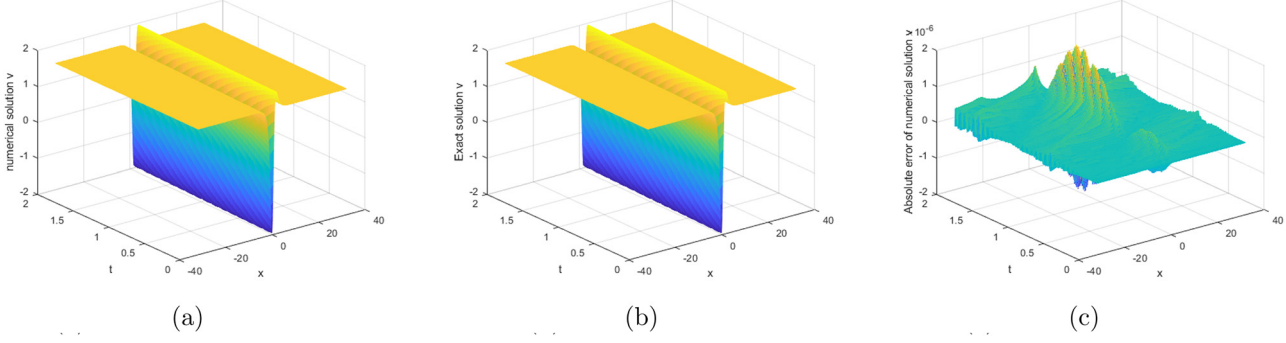

Figure 2: Comparison of numerical and exact solutions at $c = 1, a = 1, \gamma = 2, \beta = 0.9, L = 64, N = 512$. (a) Numerical solution $\mathbf{v}$, (b) exact solution $\mathbf{v}$, and (c) absolute error of $\mathbf{v}$.

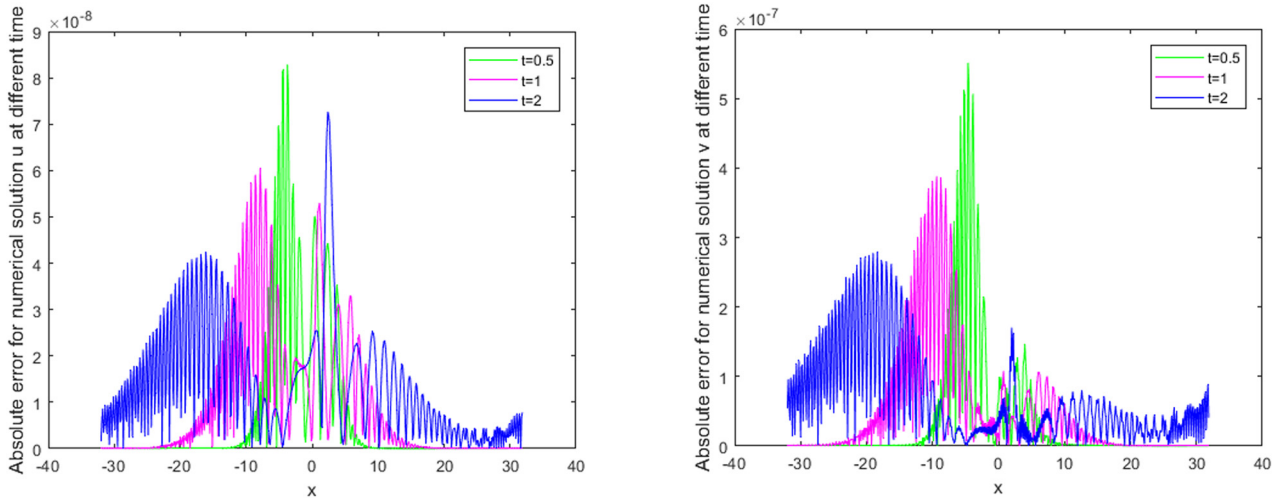

Figure 3: Absolute error at different times t.

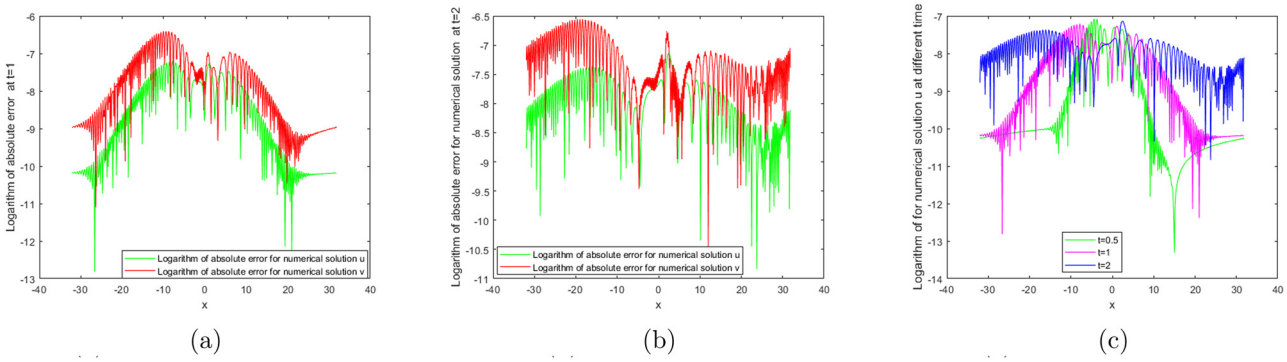

Figure 4: Logarithmic of absolute error at different times t. (a) $t = 1$, (b) $t = 2$, and (c) logarithmic of absolute error of u.

set $c = 1, a = -1, \gamma = -2, \beta = 0.9, L = 64, N$ =512, $h = 0.01$. Comparisons of numerical and exact solutions are shown in Figures 1 and 2. Logarithmic of absolute error and absolute error at different times t are shown in Figures 3 and 4.

From Figures 1–4, Fourier spectral method for the fractional-in-space coupled WBK equation is efficient and highly accurate. Next we observe the influence of fractional-orders on fractal solitary wave propagation of the fractional WBK equation.

We set $c = 1, a = -1, \gamma = -2, \beta = 0.9, L = 64, N = 512$, and different fractional-order derivatives $\alpha_1 = 0.95$, 0.9, 0.6, 0.3. Fractal solitary wave propagation of the fractional WBK equation is shown in Figures 5 and 6. Figure 5 shows fractal solitary wave propagation about u at different fractional-order derivatives α_1. Figure 6 shows fractal solitary wave propagation about v at different fractional-order derivatives α_1.

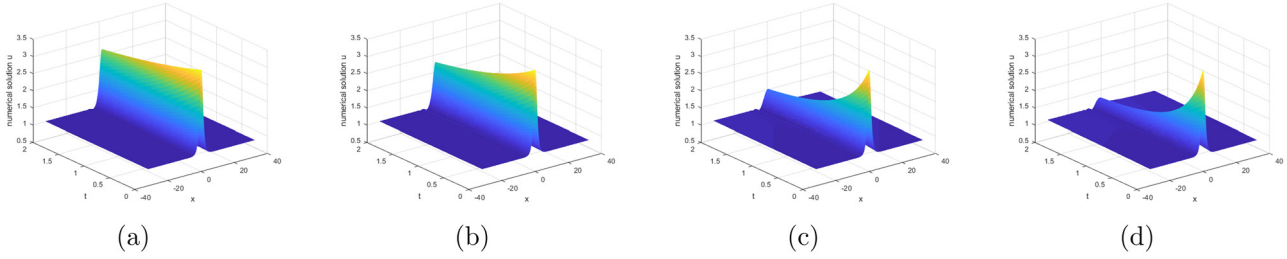

Figure 5: Fractal solitary wave propagation about u at different fractional-order derivatives α_1. (a) $\alpha_1 = 0.95$, (b) $\alpha_1 = 0.9$, (c) $\alpha_1 = 0.6$, and (d) $\alpha_1 = 0.3$.

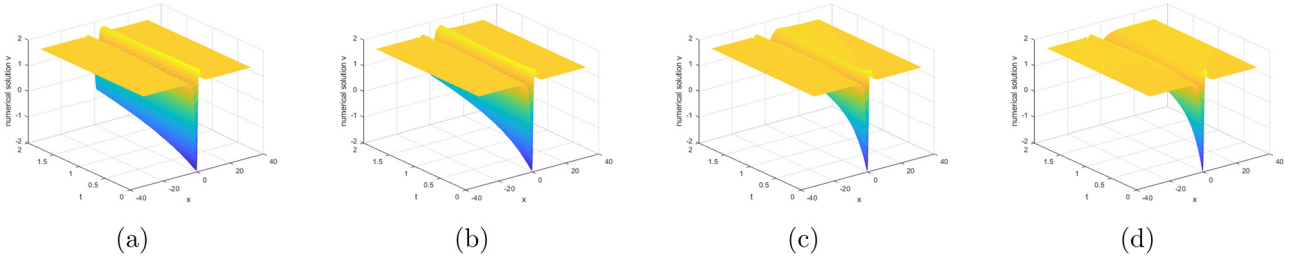

Figure 6: Fractal solitary wave propagation about v at different fractional-order derivatives α_1. (a) $\alpha_1 = 0.95$, (b) $\alpha_1 = 0.9$, (c) $\alpha_1 = 0.6$, and (d) $\alpha_1 = 0.3$.

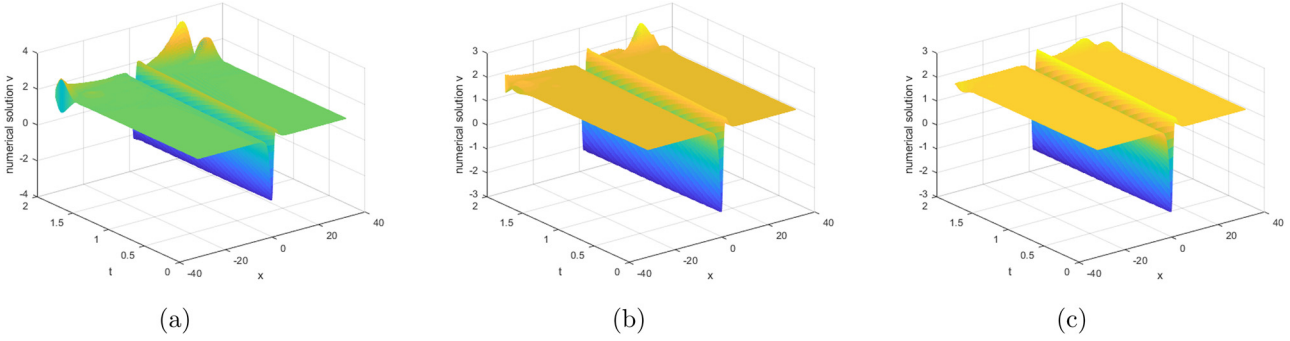

Figure 7: Fractal solitary wave propagation about v at different fractional-order derivatives α_2. (a) $\alpha_2 = 0.99$, (b) $\alpha_2 = 0.9905$, and (c) $\alpha_2 = 0.991$.

From Figures 5 and 6, we can find the wave crest changes with the change in fractional-order derivative α_1, and if fractional-order derivative α_1 is smaller, the peak value of the corresponding wave crest is smaller. Next we observe the influence of fractional-order derivative α_2 on fractal solitary wave of the fractional WBK equation.

We set $c = 1$, $a = -1$, $\gamma = -2$, $\beta = 0.9$, $L = 64$, $N = 512$, and different fractional-order derivatives $\alpha_2 = 0.99, 0.9905, 0.991$. Fractal solitary wave propagation of the fractional WBK equation about v is shown in Figure 7.

From Figure 7, we can find the fractal solitary wave propagation turn into singular soliton wave propagation. Next we observe the influence of fractional-order derivatives α_3, α_4 on fractal solitary wave of the fractional WBK equation.

We set $c = 1$, $a = -1$, $\gamma = -2$, $\beta = 0.9$, $L = 64$, $N = 512$, and different fractional-order derivatives $\alpha_4 = 0.9966, 0.9969$.

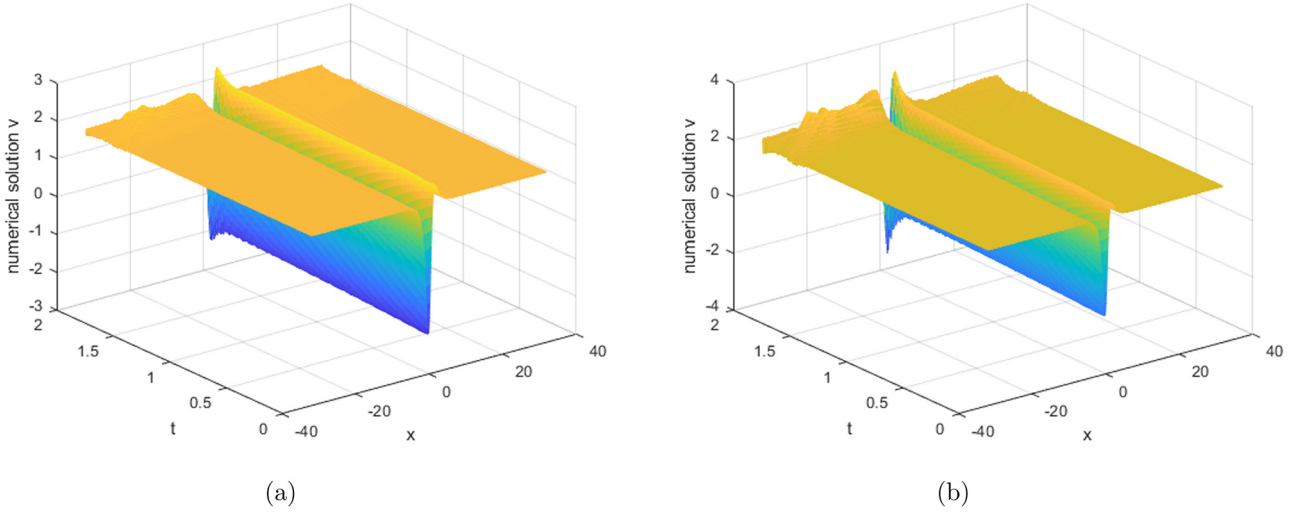

Figure 8: Fractal solitary wave propagation about v at different fractional-order derivatives α_3. (a) $\alpha_3 = 0.994$ and (b) $\alpha_3 = 0.9935$.

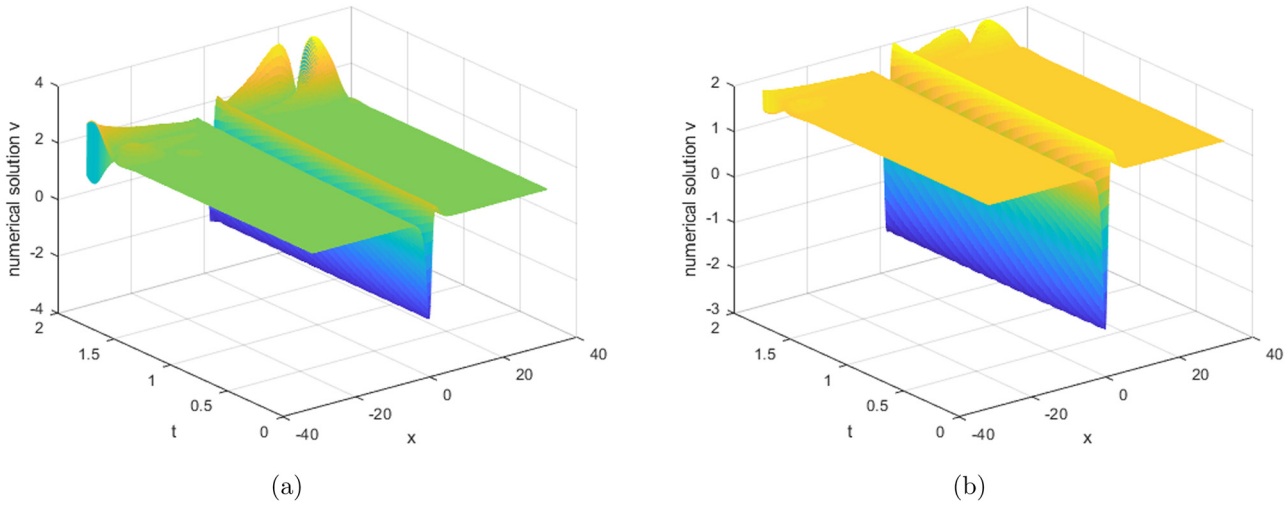

Figure 9: Fractal solitary wave propagation about v at different fractional-order derivative α_4. (a) $\alpha_4 = 0.9966$ and (b) $\alpha_4 = 0.9969$.

Fractal solitary wave propagation of the fractional WBK equation about v is shown in Figure 9.

We set $c = 1$, $a = -1$, $\gamma = -2$, $\beta = 0.9$, $L = 64$, $N = 512$, and different fractional-order derivatives $\alpha_3 = 0.994, 0.9935$. Fractal solitary wave propagation of the fractional WBK equation about v is shown in Figure 8.

In this study, we investigate the influence of fractional orders on fractal solitary wave propagation of the space fractional coupled WBK equation.

4 Conclusion

The Fourier spectral method is applied successfully to solve the fractional WBK equation and the influence of different fractional-order derivatives on wave propagation of the fractional WBK equation is investigated. From the experiment, we find that if $\alpha \longrightarrow 1$, then the numerical solution of the space fractional coupled WBK equation agrees with the exact solution of integer coupled WBK equation and the solution of the space fractional coupled WBK equation is sensitive to change in fractional orders. We observe that the fractal anomalous transmission of wave propagation of the nonlinear the space fractional coupled WBK equation changes as different fractional derivatives. Some novel anomalous transmission of the space fractional coupled WBK equation is shown by the numerical simulation. The fractional WBK equations can describe a variety of complex physical phenomena, such as wave propagation in fluid, interaction of solitons, *etc*. The numerical methods presented in this study can simulate the behavior of these phenomena under different conditions and help us better understand the physical processes.

Funding information: This study was supported by Doctor innovation research fund project of Jining Normal University (jsbsjj2355), Doctoral research start-up fund of Inner Mongolia University of Technology (DC2300001252), and the Natural Science Foundation of Inner Mongolia (2024LHMS06025).

Author contributions: conceptualization, Li-Fang Zhao; methodology and software, Li-Fang Zhao and Wei Zhang; data curation, formal analysis and funding acquisition, Wei Zhang; validation, Li-Fang Zhao; writing – original draft and writing – review and editing, Li-Fang Zhao and Wei Zhang. All authors have accepted responsibility for the entire content of this manuscript and approved its submission.

Conflict of interest: The authors state no conflict of interest.

Data availability statement: The datasets generated and/or analysed during the current study are available from the corresponding author on reasonable request.

References

[1] Yaslan HC. New analytic solutions of the space–time fractional Broer-Kaup and approximate long water wave equations. J Ocean Eng Sci. 2018;3(4):295–302.

[2] Guo SM, Mei LQ, Li Y, Sun YF. The improved fractional sub-equation method and its applications to the space–time fractional differential equations in fluid mechanics. Phys Lett A. 2012;376(4):407–11.

[3] Zaman UHM, Arefin MA, Akbar MA, Uddin MH. Analytical behavior of soliton solutions to the couple type fractional-order nonlinear evolution equations utilizing a novel technique. Alexandria Eng J. 2022;61(12):11947–58.

[4] Guo S, Zhou Y. The extended G'G-expansion method and its applications to the Whitham–Broer–Kaup–Like equations and coupled Hirota–Satsuma KdV equations. Appl Math Comput. 2010;215(9):3214–21.
[5] Zheng Z, Shan WR. Application of Exp-function method to the Whitham-Broer-Kaup shallow water model using symbolic computation. Appl Math Comput. 2009;215(2):2390–6.
[6] Ghehsareh HR, Majlesi A, Zaghian A. Lie symmetry analysis and conservation laws for time fractional coupled Whitham-Broer-Kaup equations. UPB Sci Bull, Ser A: Appl Math Phys. 2018;80(3):153–68.
[7] Saha RS. A novel method for travelling wave solutions of fractional Whitham-Broer-Kaup, fractional modified Boussinesq and fractional approximate long wave equations in shallow water. Math Methods Appl Sci. 2015;38:1352–68.
[8] Wazwaz AM. Partial differential equations and solitary waves theory. Berlin, Germany: Springer Science & Business Media; 2010.
[9] Ali A, Shah K, Khan RA. Numerical treatment for traveling wave solutions of fractional Whitham-Broer-Kaup equations. Alexandria Eng J. 2018;57(3):1991–8.
[10] Chen Y, Wang Q, Li B. A generalized method and general form solutions to the Whitham-Broer-Kaup equation. Chaos Solitons Fractals. 2004;22(3):675–82.
[11] Abdou MA. The extended tanh method and its applications for solving nonlinear physical models. Appl Math Comput. 2007;190(1):988–96.
[12] Song M, Cao J, Guan X. Application of the bifurcation method to the Whitham-Broer-Kaup-Like equations. Math Comput Model. 2012;55(3):688–99.
[13] Xu G, Li Z. Exact travelling wave solutions of the Whitham-Broer-Kaup and Broer-Kaup-Kupershmidt equations. Chaos Solitons Fractals. 2005;24(2):549–56.
[14] Lin GD, Gao YT, Gai XL, Meng DX. Extended double Wronskian solutions to the Whitham-Broer-Kaup equations in shallow water. Nonlinear Dyn. 2011;64(1):197–206.
[15] Lei W, Gao YT, Gai XL. Gauge transformation, elastic and inelastic interactions for the Whitham-Broer-Kaup shallow-water model. Commun Nonlinear Sci Numer Simul. 2012;17(7):2833–44.
[16] Xu T. Darboux transformation and new multi-Soliton solutions of the Whitham-Broer-Kaup equations. Appl Math. 2015;6(1):20–27.
[17] Fan E, Zhang H. Backlund transformation and exact solutions for Whitham-Broer-Kaup equations in shallow water. Appl Math Mech. 1998;19(8):713–6.
[18] Yan Z, Zhang H. New explicit solitary wave solutions and periodic wave solutions for Whitham-Broer-Kaup equation in shallow water. Phys Lett A. 2001;285(5):355–62.
[19] Xie FD, Yan ZY, Zhang HQ. Explicit and exact traveling wave solutions of Whitham-Broer-Kaup shallow water equations. Phys Lett A. 2001;285(1):76–80.
[20] Xu T, Li J, Zhang HQ, Zhang YX, Yao ZZ, Tian B. New extension of the tanh-function method and application to the Whitham-Broer-Kaup shallow water model with symbolic computation. Phys Lett A. 2007;369(5):458–63.
[21] Zheng Z, Shan WR. Application of Exp-function method to the Whitham-Broer-Kaup shallow water model using symbolic computation. Appl Math Comput. 2009;215:2390–6.
[22] El-Sayed SM, Kaya D. Exact and numerical traveling wave solutions of Whitham-Broer-Kaup equations. Appl Math Comput. 2005;167:1339–49.
[23] Ganji DD, Rokni HB, Sfahani MG, Ganji SS. Approximate traveling wave solutions for coupled Whitham-Broer-Kaup shallow water. Adv Eng Softw. 2010;41:956–61.
[24] Ding HF, Liiii CP. High-order numerical algorithm and error analysis for the two-dimensional nonlinear spatial fractional complex Ginzburg-Landau equation. Commun Nonlinear Sci Numer Simul. 2023;120:107160.
[25] Gao XL, Li ZY, Wang YL. Chaotic dynamic behavior of a fractional-order financial systems with constant inelastic demand. Int J Bifurc Chaos. 2024;34(9):2450111.
[26] Gao XL, Zhang HL, Li XY. Research on pattern dynamics of a class of predator-prey model with interval biological coefficients for capture. AIMS Math. 2024;9(7):18506–27.
[27] Li ZY, Chen QT, Wang YL, Li XY. Solving two-sided fractional super-diffusive partial differential equations with variable coefficients in a class of new reproducing kernel spaces. Fractal Fract. 2022;6(9):492.
[28] Liu FF, Wang YL, Li SG. Barycentric interpolation collocation method for solving the coupled viscous Burgers' equations. Int J Comput Math. 2018;95(11):2162–73.
[29] Che H, Yu-Lan W, Zhi-Yuan L. Novel patterns in a class of fractional reaction-diffusion models with the Riesz fractional derivative. Math Comput Simulat. 2022;202:149–63.
[30] Han C, Wang YL. Numerical solutions of variable-coefficient fractional-in-space KdV equation with the Caputo fractional derivative. Fractal Fract. 2022;6(4):207.
[31] Ning J, Wang YL. Fourier spectral method for solving fractional-in-space variable coefficient KdV-Burgers equation. Indian J Phys. 2024;98(5):1727–44.
[32] Li XY, Han C, Wang YL. Novel patterns in fractional-in-space nonlinear coupled FitzHugh-Nagumo models with Riesz fractional derivative. Fractal Fract. 2022;6(3):136.
[33] Gao XL, Zhang HL, Wang YL, Li XY. Research on pattern dynamics behavior of a fractional vegetation-water model in arid flat environment. Fractal Fract. 2024;8(5):264.
[34] Han C, Wang YL, Li ZY. A high-precision numerical approach to solving space fractional Gray-Scott model. Appl Math Lett. 2022;125:107759.
[35] Li XY, Wang YL, Li ZY. Numerical simulation for the fractional-in-space Ginzburg-Landau equation using Fourier spectral method. AIMS Math. 2023;8(1):2407–18.
[36] Fu Z, Liu S, Liu S. New kinds of solutions to Gardner equation. Chaos Solitons Fractals. 2004;20(2):301–9.
[37] Wazwaz AM. New solitons and kink solutions for the Gardner equation. Commun Nonlinear Sci Numer Simul. 2007;12(8):1395–404.
[38] Akbar MA, Ali NHM. New solitary and periodic solutions of nonlinear evolution equation by Exp-function method. World Appl Sci J. 2012;17(12):1603–10.